A Motile *Chlamydomonas* Flagellar Mutant That Lacks Outer Dynein Arms

D. R. MITCHELL and J. L. ROSENBAUM
Department of Biology, Yale University, New Haven, Connecticut 06511

ABSTRACT A new *Chlamydomonas* flagellar mutant, pf-28, which swims more slowly than wild-type cells, was selected. Thin-section electron microscopy revealed the complete absence of outer-row dynein arms in this mutant, whereas inner-row arms and other axonemal structures appeared normal. SDS PAGE analysis also indicated that polypeptides previously identified as outer-arm dynein components are completely absent in pf-28. The two ATPases retained by this mutant sediment at 17.7S and 12.7S on sucrose gradients that contain 0.6 M KCl. Overall swimming patterns of pf-28 differ little from wild-type except that forward swimming speed is reduced to 35% of the wild-type value, and cells show little or no backward movement during photophobic avoidance. Mutant cells will respond to phototactic stimuli, and their flagella will beat in either the forward or reverse mode. This is the first report of a mutant that lacks dynein arms that can swim.

Analysis of flagellar mutations in *Chlamydomonas* should greatly simplify the assignment of specific functions to flagellar structures. Mutants have previously been isolated that lack either a part or all of the radial spokes (12, 22), central pair microtubule complex (1, 17, 22), inner dynein arms (9), and outer dynein arms (9). A correlation between alterations in flagellar motility and lack of a particular structure has not been possible, however, because all of these mutants are virtually paralyzed. This suggests that all of the above-mentioned structures are required for motility, and a defect in any one renders the entire system inoperative. An alternative explanation may be that previous investigations specifically selected nonmotile mutants, and hence may have selected mutations with pleiotropic effects on motility as well as structure. The recent discovery of extragenic suppressors of mutations without radial spokes and central pairs (4) supports this conclusion, since these suppressors restore partial motility without restoring the missing structures. This led us to search for new mutations that alter normal motile behavior without causing complete paralysis, in hopes that specific changes in motility might be correlated with specific structural defects. This paper describes a new mutant that can swim despite the absence of outer-row dynein arms. Analysis of the motility of this mutant indicates that a broad range of beat patterns can be sustained by inner-row arms alone, and that only beat frequency, bend amplitude during reversal, and overall swimming speed appear to be affected directly by the lack of outer-row dynein arms.

MATERIALS AND METHODS

Materials: Sedimentation standards thyroglobulin and catalase were purchased from Pharmacia Fine Chemicals (Piscataway, NJ), and Epon 812, glutaraldehyde, and OsO_4 from Electron Microscopy Sciences (Fort Washington, PA). All other chemicals were obtained from Sigma Chemical Co. (St. Louis, MO).

Mutagenesis and Selection: Wild-type *Chlamydomonas* strain 137c mt^+ was mutagenized by irradiation from a 15 W ultraviolet lamp at a distance of 12 cm for 6 min. After mutagenesis, cells were spread on 0.8% agar plates containing M medium (medium I of Sager and Granick, reference 18), and colonies with a diameter smaller than that typical of wild-type colonies were transferred to liquid culture for further analysis. In addition to many mutants that totally lack flagella or have completely paralyzed flagella, a few were selected that displayed motility patterns different from those of wild-type cells. One such mutant is the subject of this paper.

Tetrad Analysis: Gametogenesis was induced in M medium without nitrogen (M–N), cells were mated, and zygotes were matured in the light on M–N plates (18, 20). Zygotes were transferred to 4% agar + M plates for germination and dissection of tetrad products. Tester strains of *Chlamydomonas* that contain linkage group marker mutations were obtained from Dr. E. Harris, *Chlamydomonas* Genetics Center, Duke University. Before linkage group analysis, new mutants were backcrossed repeatedly with wild-type cells to improve meiotic viability and to ensure that the observed motility phenotype resulted from a single mutation.

Dark-field Microscopy: To analyze the speed and pattern of forward swimming, cells were grown for 3 d in M medium to a density of $\sim 10^7$ cells/ml and were photographed under constant illumination from a 60-W tungsten source by use of the dark-field setting of a Zeiss phase condenser. Illumination was adjusted to provide greatest intensity from one direction, which induced positive phototaxis of cells in the observed field. To record a relatively synchronous phototactic response over the entire field of observation, cells were dark-adapted for 30 s and then illuminated for 5 s before they were photographed.

THE JOURNAL OF CELL BIOLOGY · VOLUME 100 APRIL 1985 1228–1234

1-s exposures were made on TRI-X film at a magnification of 27. Swimming speeds were estimated by the measurement of the path length of swimming traces on prints at a final magnification of 120.

For analysis of flagellar waveforms, cells were trapped between the slide and coverslip in a thin layer of medium and were thus prevented from moving rapidly or leaving the focal plane. Flagellar waveforms were recorded as multiple exposures with stroboscopic illumination provided by a Strobex lamp and Strobex model 236 power supply (Chadwick-Helmuth Co., Inc., El Monte, CA). Photographs were made on TRI-X film with dark-field illumination provided by an Olympus dark-field condenser and a Zeiss 40× neofluar lens (0.75 numerical aperture).

Flagellar Reactivation: The isolation and demembranation of flagella, and the preparation of slides and reactivation solutions, followed the methods of Witman et al. (22). Axonemes were reactivated by a 1:50 dilution into reactivation solutions containing 1 mM ATP, 30 mM HEPES, 5 mM $MgSO_4$, 1 mM dithiothreitol, 25 mM KCl, and EDTA and $CaCl_2$ to produce free Ca^{++} concentrations in the range of 10^{-8} to 10^{-3} M (2, 22).

Electron Microscopy: Samples of flagella and axonemes were fixed at 0°C in 1% glutaraldehyde for 1 h, washed, and post-fixed in 1% OsO_4 for 1 h before dehydration and embedding in Epon 812. Fixatives were buffered with 30 mM cacodylate, 5 mM $MgSO_4$, pH 7.4. Thin sections were stained with uranyl acetate and lead citrate, and examined on a Philips 201 electron mciroscope (Philips Electronic Instruments, Inc., Mahwah, NJ) operated at 80 kV.

Isolation and Fractionation of Flagella: Cells were grown to ~5 × 10^7 cells/ml in M medium supplemented with sodium acetate. The cells were concentrated on a Pellicon filter (Millipore Corp., Bedford, MA), washed, and deflagellated with 4 mM dibucaine in 10 mM HEPES, 5 mM $MgSO_4$, 1 mM phenylmethylsulfonyl fluoride, and 2.5% sucrose. Flagella were demembranated in 0.25% Nonidet P-40 in HMDEKP[1] (10 mM HEPES, 5 mM $MgSO_4$, 0.1 mM dithiothreitol, 0.1 mM EDTA, 25 mM KCl, 1 mM phenylmethylsulfonyl fluoride, 5 μM peptstatin, pH 7.4), washed in HMDEKP, and extracted with 0.6 M KCl in HMDEKP for 20 min on ice. Extracted axonemes were spun at 35,000 *g* for 30 min, and the dynein-containing supernatant was saved. Before sucrose gradient analysis, this supernatant fraction (the KCl extract) was dialyzed against 0.1× HMDEKP for 4 h at 4°C and spun at 35,000 *g* for 30 min to remove a large portion of the nondynein protein, which is insoluble at low ionic strength (data not shown). The dialyzed KCl extract was layered onto a linear 0–20% sucrose gradient containing 0.6 M KCl in HMDEKP. Gradients were spun at 37,000 rpm for 12 h at 4°C in an SW 41 rotor (Beckman Instruments, Palo Alto, CA) and collected in 0.36-ml fractions from the bottom of the tube. Bovine liver catalase (11.3S; reference 13) and bovine thyroglobulin (~19.2S at pH 7.4; reference 6) were run on separate gradients as sedimentation standards.

ATPase and Protein Assays: ATPase activity was assayed in 40 mM HEPES, 5 mM $MgSO_4$, 0.1 mM EDTA, 25 mM KCl, 1 mM ATP, pH 7.4, at 20°C. The inorganic phosphate released over the indicated time interval was measured by the method of Taussky and Shorr (19). When sucrose gradient fractions were assayed, the enzyme samples contained 0.6 M KCl. The inclusion of 10-μl samples (wild-type dyneins) or 50-μl samples (pf-28 dyneins) in the 0.5-ml assay volume increased final KCl concentrations to 37 or 85 mM, respectively. Protein concentrations were estimated by the Bradford dye binding method (3) by use of ovalbumin as a standard.

SDS PAGE: Samples were prepared and run by using the Tris-glycine-buffering system of Laemmli (11). Stacking gels (4% acrylamide) and separating gels (4–8% acrylamide) were prepared from stocks that contained 30% acrylamide and 0.4% bis-acrylamide. Separating gels also contained 3 M urea and a 0–10% glycerol gradient. Gels were either stained with Coomassie Blue or silver stained by the procedure of Wray (23) as indicated. Myosin (205,000), phosphorylase B (97,500), bovine serum albumin (66,000), aldolase (40,000), and soybean trypsin inhibitor (20,100) were used as molecular weight standards.

RESULTS

Mutant Selection

The mutant described in this paper, pf-28, was initially selected on the basis of small colony size on 0.8% agar + M medium, and was then observed to swim at a reduced speed in liquid culture. It was subcloned, and a representative clone was repeatedly backcrossed to the wild-type parent of opposite mating type. Colony morphology and swimming phenotype were found to co-segregate 2:2 with wild-type, which indicates that the alteration in motility is the result of a single Mendelian mutation. Tetrad analysis has shown that pf-28 is not in linkage groups I or IX, and is thus not allelic to pf-22 or pf-13, the other outer-arm dynein mutations (9). The genetic markers used and the resulting tetrad ratios (parental ditype/nonparental ditype/tetratype) were msr-1 (1:1:10), ery-3 (1:1:10), and pf-22 (2:3:1) for linkage group I, and sr-1 (3:2:6) for linkage group IX. The genetic locus of this mutation has not as yet been mapped.

Swimming Phenotype

The swimming pattern and velocity of pf-28 cells were compared with those of wild-type cells using dark-field light microscopy. As illustrated in Fig. 1, both cell types generate a gently waving trace which results from the helical swimming path typical of normal forward swimming (10). The pf-28 cells, however, move only one-third as far as the wild-type cells during a 1-s exposure. Measurement of swimming traces such as those in Fig. 1 gave an estimated speed of 215 ± 14 μm/s (mean ± SD; n = 30) for wild-type cells and 76 ± 5 μm/s (n = 30) for pf-28 cells. Except for this difference in swimming speed, no obvious differences in swimming patterns of the two cell types were noted.

The beat frequency of live, swimming cells was estimated to determine whether the noted reduction in swimming speed was correlated with a lower beat frequency. Cells were observed under strobe illumination, and the flash rate was adjusted to match the beat frequency of individual cells. Wild-type cells of strain 137c swam with an average frequency of 40 Hz, whereas the beat frequency of pf-28 cells was only 22 Hz under the same conditions. Thus, the slower swimming speed of mutant cells is largely due to a 45% reduction in beat frequency.

Electron Microscopy

Demembranated axonemes from pf-28 and wild-type cells were prepared for thin-section electron microscopy as described above. Examination of a large number of transverse sections of pf-28 axonemes, as seen in Fig. 2, *a* and *c*, revealed the complete lack of outer-row dynein arms in this mutant, whereas outer-row arms are easily seen in wild-type axonemes (Fig. 2*d*, arrowhead). Electron-dense material at an outer-arm location was observed on one doublet per axoneme in 28 of 88 cross-sections of pf-28 axonemes. In most cases, this material was identified as the interdoublet bridge, previously described by Hoops and Witman (8), which replaces outer-row arms along one doublet of wild-type flagella (arrows, Fig. 2*a*). Analysis of longitudinal sections also supports the conclusion that no outer-row arms are present in pf-28, since outer-row arms are clearly visible along wild-type doublets (Fig. 2*f*), but periodic structures that resemble outer-row arms are never observed along pf-28 doublets (Fig. 2*e*). To test for the potential loss of a labile outer-arm structure during axoneme preparation, freshly isolated flagella were also fixed and prepared for thin-section electron microscopy. Although resolution was reduced by the dense flagellar matrix, inner arms were visible but no outer arms were seen (Fig. 2*b*).

The morphology of inner-row dynein arms in pf-28 axonemes was indistinguishable from that of wild-type inner arms, at the resolution available in thin sections. In cross-

[1] *Abbreviations used in this paper*: HMDEKP, a solution containing HEPES, $MgSO_4$, dithiothreitol, EDTA, KCl, phenylmethylsulfonyl fluoride, and pepstatin; HMW, high molecular weight.

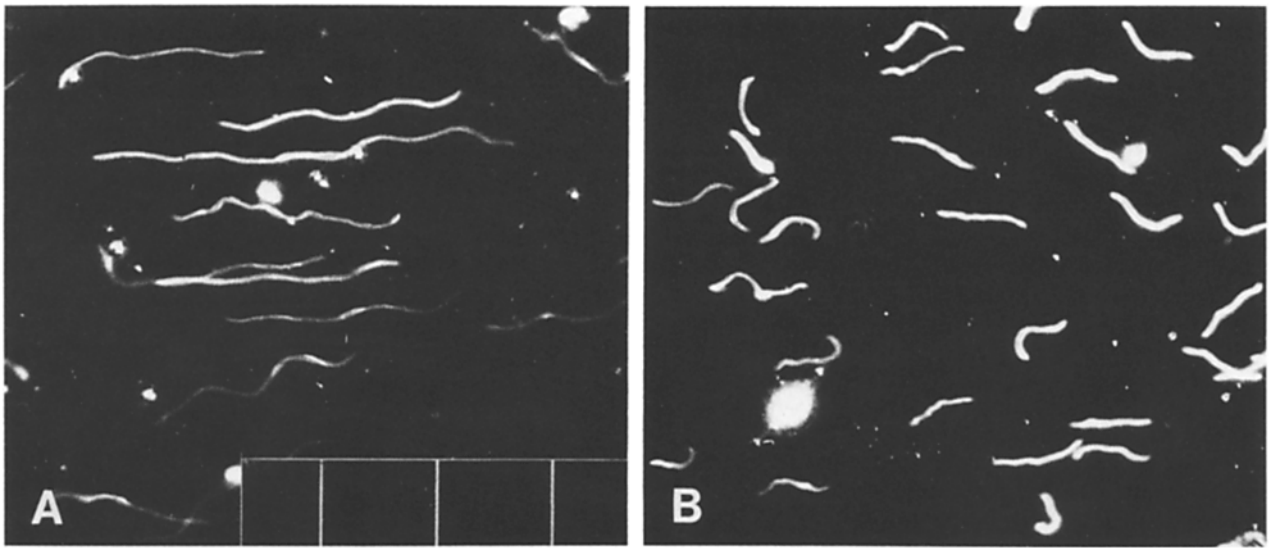

FIGURE 1 Dark-field micrographs of wild-type cells (*A*) and pf-28 cells (*B*) swimming in M medium were made with 1-s exposures on TRI-X film. Each wavy line is the path traversed by a single cell during the exposure. Most cells in both *A* and *B* are swimming toward the right-hand edge of the field. Bars, 100 μm.

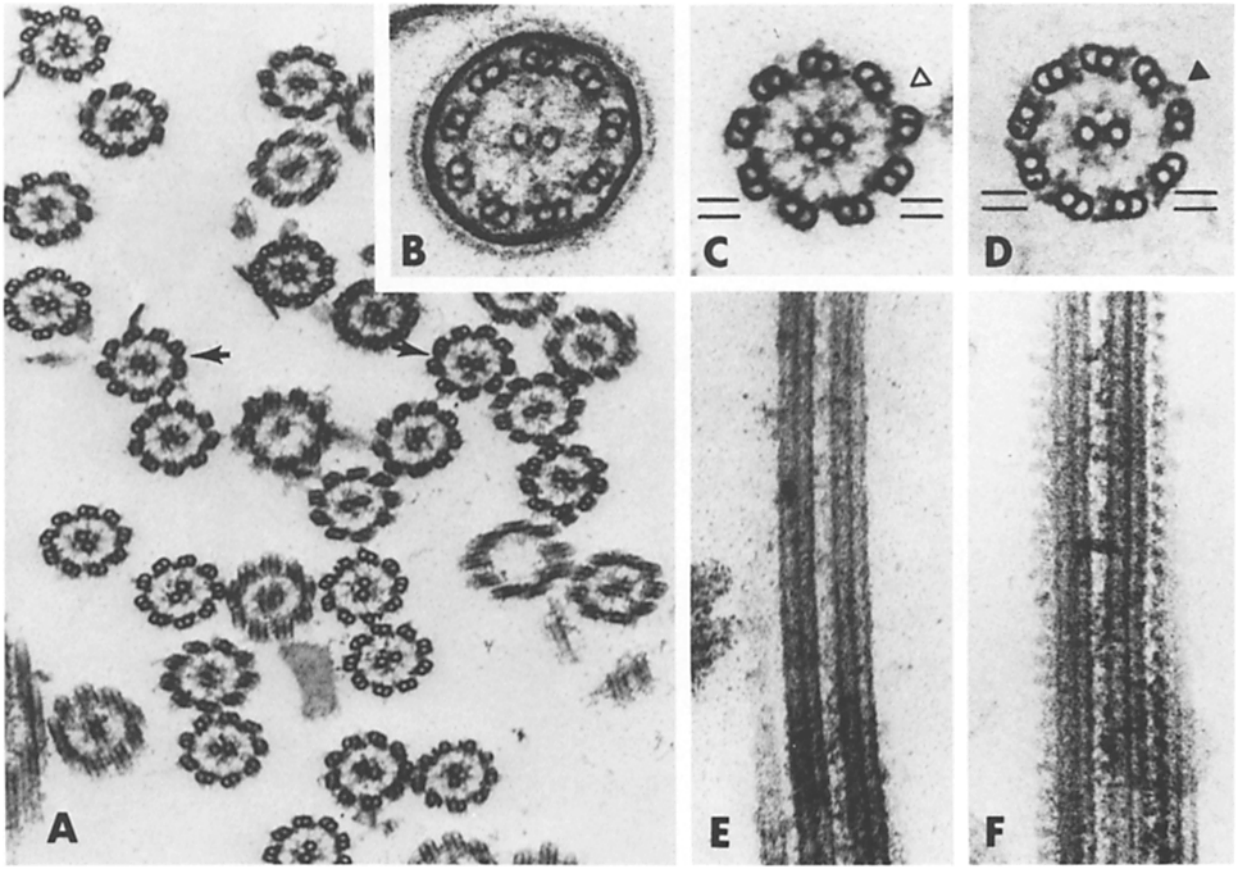

FIGURE 2 Thin-section electron micrographs of pf-28 (*A*, *C*, *E*) and wild-type (*D*, *F*) axonemes, and pf-28 flagella (*B*). Typical outer-row arms (*D*, filled arrowhead) are missing from both axonemes (*A*, *C*) and flagella (*B*) of pf-28. The open arrowhead in *C* indicates a vacant outer-arm position. Interdoublet bridges, occasionally visible on one doublet per axoneme, are retained in pf-28 (arrows in *A*; see text for details). The approximate locations of the grazing longitudinal sections seen in *E* and *F* are indicated by parallel lines in *C* and *D*. Highly periodic outer-row arms project from the edges of two wild-type doublets (*F*) but are missing in pf-28 (*E*). Inner-row arms spanning the region between the two doublets are best visualized by sighting along the doublets (*E* and *F*). (*A*) × 54,000; (*B–F*) × 118,000.

sections (Fig. 2, *c* and *d*), the inner-row arms appear as electron densities projecting from the inner edge of the A-tubule of each outer doublet into the lumen of the axoneme. Unlike outer row arms, which form cross-bridges in 5 mM $MgSO_4$ similar to those previously described in mussel gill cilia (21), inner arms rarely appeared to interact directly with

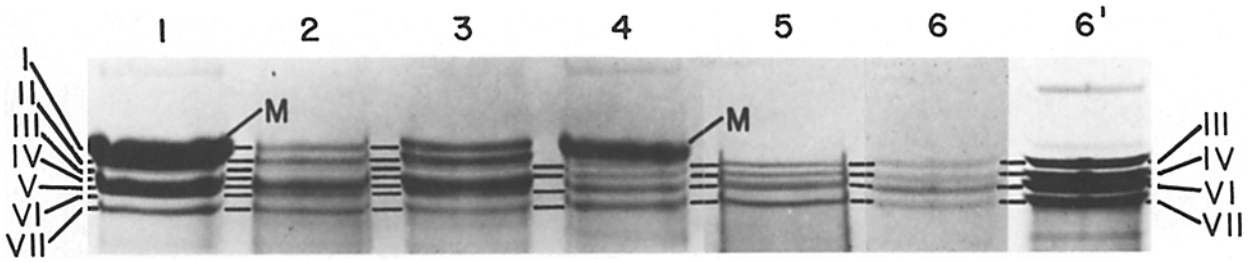

FIGURE 3 A 4–8% acrylamide, 3 M urea slab gel of wild-type (lanes *1–3*) and pf-28 (lanes 4–6, 6′) flagellar fractions. Lanes *1* and *4*, whole flagella; lanes *2* and *5*, axonemes; lanes *3* and 6, KCl extracts; all stained with Coomassie Blue. Lane 6′ shows lane 6 after staining by the more sensitive silver-stained method. The dynein bands are labeled with roman numerals. *M*, membrane protein. Only the high molecular weight region of the gel is shown.

the B-tubule of an adjacent doublet under the fixation conditions used. The similarity in electron density of the inner and outer rows of dynein arms, as viewed in cross-sections of wild-type axonemes, suggests that they contain an approximately equal mass per unit length of axoneme. In longitudinal sections, however, there are differences in the appearance of inner- and outer-row dynein arms. Whereas outer-arm material is distributed in discrete electron densities separated by electron lucent spaces (Fig. 2*f*), inner-arm material is more evenly distributed along the A-tubule (Fig. 2, *e* and *f*).

Gel Electrophoresis

To determine which proteins were missing from pf-28 flagella, samples were prepared for SDS PAGE. Since complete resolution of the multiple high molecular weight (HMW) dynein bands cannot be achieved with the Tris-glycine buffering system of Laemmli (11), we modified the separating gel by adding 3 M urea. This greatly improves the resolution of dynein at protein loads sufficient for Coomassie Blue staining, but alters the mobility of some bands. Molecular weights were therefore estimated by use of gels run without urea. Coomassie Blue–stained gels of flagella, axonemes, and a 0.6 M KCl extract of axonemes from wild-type and pf-28 cells (Fig. 3) show that three prominent HMW proteins are missing in the mutant without outer arms. These three proteins correspond to bands I, II, and V of Piperno and Luck (15) and have been previously identified as outer-arm components (9, 15). They could not be detected in pf-28 KCl extracts even after sensitive silver staining of the gel (Fig. 3, lane 6′). All of the other previously identified outer-arm dynein polypeptides, with molecular weights of 83,000, 70,000, and 15,000–20,000, are also absent (not shown).

Several HMW proteins are retained by pf-28 flagella (Fig. 3, lane *4*), and are thus presumed to be proteins of the inner dynein arm. Detergent extraction removes the major membrane glycoprotein, improving the resolution of HMW dynein bands in axonemal samples (Fig. 3, lanes *3* and *5*) and revealing four prominent HMW bands in pf-28 axonemes and KCl extracts: bands III, IV, VI, and VII in order of decreasing molecular weight. (The nomenclature used here probably corresponds directly to that of Piperno and Luck (15), although an exact comparison using the same electrophoretic techniques has not been performed.) The apparent stoichiometry of these bands, assuming equivalent Coomassie Blue binding, is 1:1:2:2 in flagella and axonemes but only 1:1:2:1 in KCl extracts. Only half of band VII is extracted, which suggests that band VII (and possibly band VI as well) may consist of two nonidentical proteins that co-migrate in our gel system.

TABLE I
Mg-ATPase Activity

Fraction	Specific activity	
	Wild-type	pf-28
	μmol inorganic P/mg per min	
Axonemes	0.27	0.05
KCl extract	0.39	0.07
20S (fraction 6)	1.67	—
12S (fraction 16)	0.38	—
17.7S (fraction 8)	—	0.07
12.7S (fraction 15)	—	0.04

Values for axonemes and KCl extracts are averages from two experiments. Value for ATPase peaks are individual measurements calculated from the data presented in Fig. 4.

ATPase Activity and Sucrose Gradient Analysis

The ATPase activity and protein content of these flagellar fractions were tested to determine the fraction of the total Mg-ATPase activity contributed by inner- and outer-row arms (Table I). The specific activity of pf-28 axonemes (presumed to consist solely of inner arm dynein) was only 18% of that of wild-type axonemes (inner- and outer-arm dyneins). To normalize the data from wild-type and mutant axonemes, total axonemal ATPase activity was divided by the amount of protein left in the outer-doublet fraction which followed KCl extraction. This generates a relative measure of the ATPase activity per axoneme and shows that only 12% of the total (wild-type) activity is contributed by inner-row arms (pf-28 activity) under the assay conditions employed.

ATPases were further purified by sucrose density gradient centrifugation, and fractions were analyzed for protein concentration and ATPase activity. These gradients were run in the presence of 0.6 M KCl to minimize nonspecific protein-protein interactions. Thyroglobulin (19.2S) and catalase (11.3S) were run on identical gradients as sedimentation standards, but since the effect of high ionic strength on the sedimentation rates of these standards is not known, the apparent sedimentation coefficients can only be used as rough approximations of true sedimentation rates. KCl extracts of wild-type axonemes contain two major ATPases with apparent sedimentation rates under these conditions of 20S and 12S (Fig. 4*a*), which correspond to the 18S and 12S outer-arm ATPases previously described (14, 15). Inner-arm ATPase activity cannot be detected in gradients of wild-type dyneins (see below), but is apparent in KCl extracts from pf-28 axonemes that contain two major ATPases with apparent sedimentation coefficients of 17.7S and 12.7S (Fig. 4*b*). The latter values will be used as provisional designations until more accurate measurements can be made. One should note

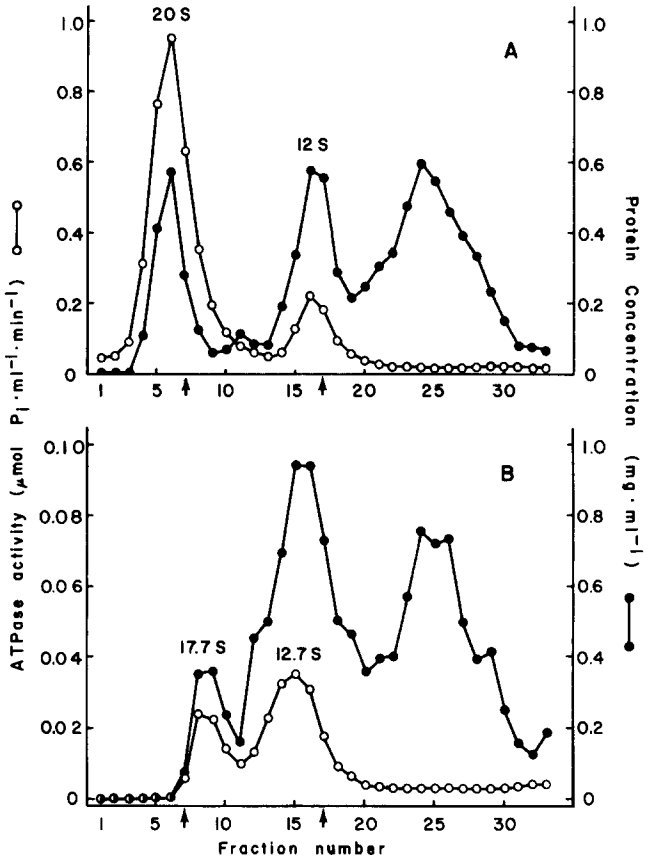

FIGURE 4 Sucrose gradient profiles of (*A*) wild-type and (*B*) pf-28 KCl extracts prepared from 20 liters of wild-type cells and 40 liters of pf-28 cells, respectively. Protein concentration is shown to the same scale in *A* and *B*, but ATPase scales differ 10-fold. Although wild-type KCl extracts contain both inner- and outer-arm dyneins, only the high specific activity outer-arm dyneins (*20S* and *12S*) are visible in *A*. KCl extracts from pf-28 axonemes (*B*) contain only the low specific-activity inner-arm ATPases that sediment at *17.7S* and *12.7S* under our conditions. Extracts were loaded onto 0–20% sucrose gradients containing HMDEKP and 0.6 M KCl, and spun in an SW 41 rotor at 37,000 rpm for 12 h. Arrows on the abscissa show the location of sedimentation standards thyroglobulin (19.2S) and catalase (11.3S).

that the ATPase activity scale in Fig. 4*b* is expanded 10-fold from that in Fig. 4*a*, although protein concentrations are reported at the same scale. The specific activities of peak gradient fractions for each ATPase are listed in Table I. Under standard conditions, the inner-arm dyneins have extremely low specific activities (0.07 μmol inorganic P/mg per min for 17.7S dynein and 0.04 μmol inorganic P/mg per min for 12.7S dynein), which accounts for the inability to detect these enzymes in gradients of wild-type dyneins. Values for the specific activities of wild-type 20S and 12S dyneins are similar to those reported by other investigators (14, 15).

Flagellar Waveform

Flagellar waveforms of wild-type and pf-28 flagella were compared to determine whether a lack of outer-row arms alters the normal beat pattern (diagrammed in Fig. 5*a*) during either forward (asymmetrical) or reverse (symmetrical) beating. Multiple-flash images of living cells revealed very similar waveforms during normal forward swimming of wild-type (Fig. 5*b*) and pf-28 (Fig. 5*c*) cells. Beat patterns of both strains

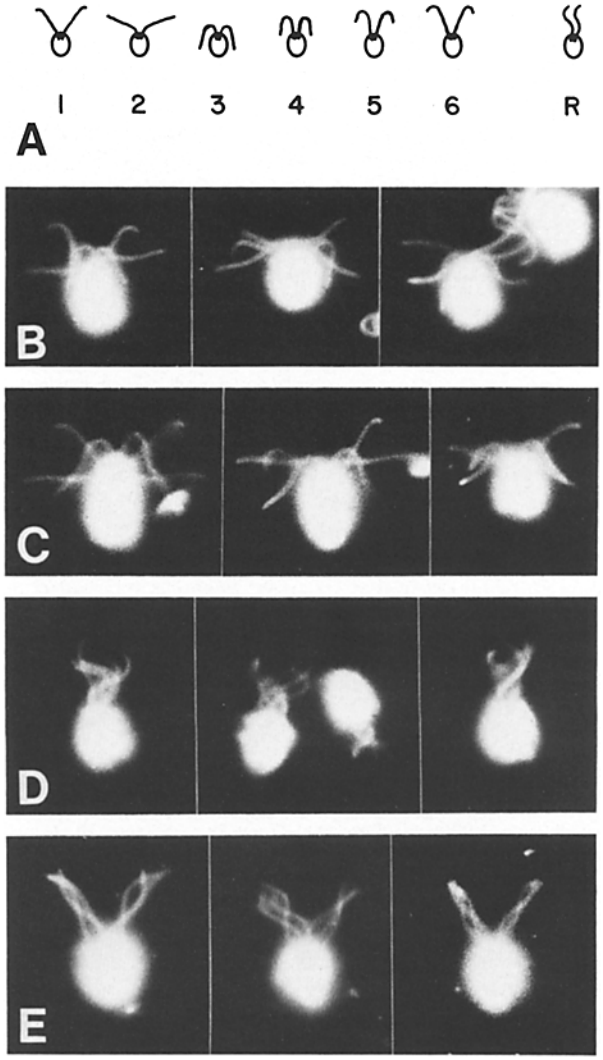

FIGURE 5 Flagellar waveform of live cells. Cells swimming in M medium were photographed under stroboscopic dark-field illumination. *A*, diagram of successive stages during the effective stroke (*1* and *2*), recovery stroke (*3–6*), and flagellar reversal (*R*) of wild-type cells. Multiple-flash images of wild-type cells (*B*) and pf-28 cells (*C*) during forward swimming reveal few differences in waveform. During flagellar reversal, the beat pattern of wild-type cells (*D*) differs markedly from that of pf-28 cells (*E*). (*B–E*) Flash rate, 12 Hz; exposure, 0.25 s. × 910.

contain large, prominent principal bends and small or no reverse bends, and progress through the same effective and recovery stroke positions.

A brief period of flagellar reversal can be induced by bright illumination of *Chlamydomonas* after a period of dark adaptation (Fig. 5*d*). During this photophobic response, wild-type cells swim backward for a short distance before resuming forward motility, whereas pf-28 cells appear to freeze for a similar time interval. At high magnification, it is apparent that pf-28 flagella do pass through a transient phase of symmetrical waveform (Fig. 5*e*), but they remain in a "V" configuration during reversal and have a much smaller bend amplitude than do wild-type flagella.

For more detailed and controlled comparisons between wild-type and pf-28 flagellar waveforms, isolated axonemes were reactivated in solutions containing varying concentrations of free Ca^{++} (2). Our observations of wild-type axonemes

agree with previously published results (2, 22). In short, axonemes reactivated below 10^{-5} M Ca^{++} display a highly asymmetric beat pattern composed of a large principal bend and little or no visible reverse bend (Fig. 6*a*). At 10^{-7} M Ca^{++}, the average beat frequency of wild-type axonemes was 57 Hz, and principal bend angles ranged from 135 to 175°; reverse bends as large as 20° were occasionally recorded. These beat parameters, along with data from live cells, are summarized in Table II. As calcium concentrations were increased above 10^{-6} M, beat frequency decreased until most axonemes were quiescent at 10^{-5} M Ca^{++}. At higher calcium concentrations, axonemes resumed beating in a symmetrical mode (Fig. 6*b*) which resembled the waveform of wild-type flagella during phototactic reversal (Fig. 5*d*).

Data obtained from pf-28 axonemes reactivated in vitro are in close agreement with in vivo observations. The beat frequency of pf-28 axonemes reactivated at 10^{-7} M Ca^{++} was 26 Hz, or 45% of the wild-type frequency, whereas the waveform of pf-28 axonemes reactivated at low calcium concentration (Fig. 6*c*) differed slightly from a typical wild-type pattern in that principal bend angles were usually smaller and reverse bends were larger than wild-type controls (Table II). Mutant axonemes became quiescent at 10^{-5} M Ca^{++} and resumed symmetrical beating at higher calcium concentrations (Fig. 6*d*).

The percentage of pf-28 axonemes that could be reactivated at 10^{-4} M Ca^{++} was generally much lower than the percentage (usually 70–90%) reactivated at 10^{-7} M Ca^{++}, however, and reactivation often ceased after a few minutes of observation under these conditions. Some component of the motile machinery, involved only in reactivation at high calcium concentrations or at particular risk under those conditions, apparently has a greater lability in pf-28 axonemes. Those pf-28 axonemes that do reactivate at 10^{-4} M Ca^{++} have much smaller bend amplitudes than do wild-type axonemes at 10^{-4} M Ca^{++} (compare Fig. 6, *b* and *d*), in agreement with observations of live cells.

DISCUSSION

A new *Chlamydomonas* mutant has been isolated, pf-28, which is totally deficient in outer-row dynein arms (Fig. 2). The absence of outer-arm material in pf-28 was confirmed by SDS PAGE (Fig. 3), which revealed no outer-arm dynein polypeptides even after sensitive silver staining of the Coomassie Blue–stained gels. In contrast, the previously isolated mutants without outer arms, pf-13, pf-13a, pf-22, and pf-22a, all retain outer arms on at least 5% of their outer doublet microtubules (9). These other *Chlamydomonas* mutants without outer arms, and the only available mutant without inner arms (pf-23), have totally paralyzed flagella (9). A complete suppression of motility in flagella that lack only a single row of arms suggests that both rows must be functional to generate organized flagellar bends. On the contrary, sea urchin spermatozoan axonemes continue to beat at a reduced frequency after extraction of their outer-row arms (7), which indicates that inner-row arms have some capacity to function independently. The ability of pf-28 cells to swim at a reduced speed, but with a pattern otherwise indistinguishable from that of wild-type cells, demonstrates unequivocally that inner-

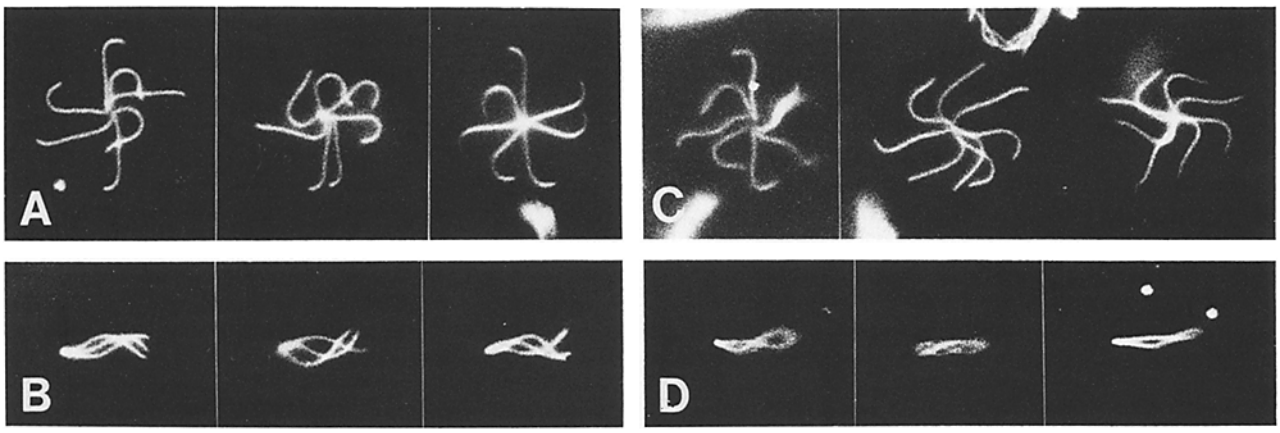

FIGURE 6 Flagellar waveform of reactivated axonemes. Multiple-flash dark-field images of reactivated axonemes from wild-type cells (*A* and *B*) and pf-28 cells (*C* and *D*) reveal only minor differences in waveform at 10^{-7} M Ca^{++} (*A* and *C*). Substantial differences in bend amplitude are seen when axonemes are beating symmetrically at 10^{-4} M Ca^{++} (*B* and *D*). (*A* and *C*) Flash rate, 6 Hz; exposure 1 s. (*B*) Flash rate, 12 Hz; exposure 0.25 s. (*D*) Flash rate, 12 Hz; exposure 0.5 s. × 1,200.

TABLE II

Swimming Parameters of Forward Motility

Parameter	Mean ± SD (*n*)	
	Wild-type	pf-28
Swimming speed of live cells (*μm/s*)	215 ± 14 (30)	76 ± 5 (30)
Beat frequency of live cells (Hz)	40 ± 6 (27)	22 ± 2 (23)
Beat frequency of axonemes (Hz)	57 ± 7 (26)	26 ± 3 (26)
Principal bend angle of axonemes (degrees)	162 ± 15 (11) (range 135–175)	119 ± 15 (17) (range 100–130)
Reverse bend angle of axonemes (degrees)	ND (range 0–20)	32 ± 5 (13) (range 25–40)

Measurements were made on live cells swimming in M medium or on axonemes reactivated in 1 mM ATP, 5 mM $MgSO_4$, 30 mM HEPES, 25 mM KCl, 4.99×10^{-4} M EDTA, 1.55×10^{-6} M $CaCl_2$, 1 mM dithiothreitol, and 0.5% polyethylene glycol 20,000 (free Ca^{++} concentration 10^{-7} M). ND, not determined.

row arms can act independently to sustain flagellar beating.

Most of the cells in Fig. 2, *a* and *b* are progressing uniformly in one direction in response to a positive phototactic stimulus (see Materials and Methods). Thus, the phototactic reorientation of pf-28 cells under these conditions does not differ from that of wild-type cells. In addition, if either wild-type or pf-28 cells are dark-adapted for 1 to 2 min, bright illumination will induce a typical reversal response (5) in which the flagella temporarily beat in a symmetrical "flagellar" mode, then resume their normal, asymmetrical "ciliary" beating mode. These results indicate that calcium-mediated changes in flagellar waveform, such as the reversal response (2, 5) and phototactic turning (10), do not require any functions provided exclusively by outer row dynein arms.

We have identified specific effects of the pf-28 mutation on flagellar beat parameters by examining both live cells and reactivated axonemes. During forward swimming, pf-28 flagella beat with an asymmetric waveform that closely resembles that of wild-type flagella, but with a frequency reduced to ~55% of the wild-type frequency. Isolated pf-28 axonemes, reactivated at 10^{-7} M Ca^{++}, also beat at only 40–50% of the wild-type frequency, and display waveforms that differ only slightly from the typical wild-type pattern. The primary effect of a lack of outer-row arms on normal forward motility is thus a reduction in beat frequency to half the normal value, a result identical to that observed previously by outer-arm extraction of sea urchin axonemes (7). Although pf-28 cells display flagellar reversal during photophobic episodes, their flagellar beat patterns differ from the typical wild-type response in two aspects. Average bend angles of wild-type flagella are considerably larger than those of pf-28 flagella, and the base of wild-type flagella are parallel during reversal, whereas those of pf-28 are held in a "V". This suggests that outer-row arms may play a direct role in flagellar reorientation during a reversal response. Alternatively, complete reorientation may require greater bend amplitudes and their resultant hydrodynamic forces.

The total absence of outer-arm components in pf-28 flagella greatly facilitates the analysis of additional dynein ATPases (presumably inner-arm components) whose presence in extracts from wild-type flagella is masked by the much higher specific activities of the outer arm ATPases. When KCl extracts of pf-28 axonemes are applied to sucrose gradients, two peaks of ATPase activity are seen, with sedimentation rates intermediate to those of the two outer-arm ATPases (Fig. 4). We have not subjected these ATPases to detailed sedimentation rate analyses, and since the conditions used in these experiments do not approximate $S_{20,w}$ conditions, we cannot assign accurate S values as yet. By assuming that high ionic strength does not alter the S values of our standards, we obtain provisional values of 17.7S and 12.7S for the sedimentation rates of the ATPases remaining in this mutant. Previous comparisons of *Chlamydomonas* wild-type ATPases with those of a mutant without inner arms, pf-23, described inner-arm dyneins with sedimentation coefficients of 10–11S and 12.5S (9, 16). A 10–11S ATPase was also isolated from wild-type flagella by Pfister et al. (14). The relationship between these previously described ATPases and the dyneins of pf-28 have not been established, although preliminary electrophoretic analysis (not shown) indicates that the polypeptides associated with our 12.7S and 17.7S activities are missing in pf-23, and that both of these ATPase complexes are therefore components of the inner-arm row.

It is clear that gross similarity in the swimming behavior of pf-28 and wild-type cells and the general equivalence of their flagellar waveforms shows that a wide range of normal motility functions are retained by pf-28 flagella. Outer arms are not required for these functions, which suggests that both arm rows may contribute little more to flagellar motility than interdoublet sliding forces, which are then controlled by other axonemal structures to generate bends.

We wish to thank Dr. Ted Clark for helpful discussions and critical reading of the manuscript.

This work was supported by National Institutes of Health fellowship GM08595 to Dr. Mitchell and National Institutes of Health grant GM14642 to Dr. Rosenbaum.

Received for publication 26 October 1984, and in revised form 13 December 1984.

REFERENCES

1. Adams, G. M. W., B. Huang, G. Piperno, and D. J. L. Luck. 1981. Central-pair microtubular complex of *Chlamydomonas* flagella: polypeptide composition as revealed by analysis of mutants. *J. Cell Biol.* 91:69–76.
2. Bessen, M., R. B. Fay, and G. B. Witman. 1980. Calcium control of waveform in isolated flagellar axonemes of *Chlamydomonas*. *J. Cell Biol.* 86:446–455.
3. Bradford, M. M. 1976. A rapid and sensitive method for the quantitation of microgram quantities of protein utilizing the principle of protein-dye binding. *Anal. Biochem.* 72:248–254.
4. Brokaw, C. J., D. J. L. Luck, and B. Huang. 1982. Analysis of the movement of *Chlamydomonas* flagella: the function of the radial-spoke system is revealed by comparison of wild-type and mutant flagella. *J. Cell Biol.* 92:722–732.
5. Eckert, R., and J. A. Schmidt. 1976. Calcium couples flagellar reversal to photostimulation in *Chlamydomonas reinhardtii*. *Nature (Lond.).* 262:713–715.
6. Edelhoch, H. 1960. The properties of thyroglobulin. I. The effects of alkali. *J. Biol. Chem.* 235:1326–1334.
7. Gibbons, B. H., and I. R. Gibbons. 1976. Functional recombination of dynein I with demembranated sea urchin sperm partially extracted with KCl. *Biochem. Biophys. Res. Commun.* 73:1–6.
8. Hoops, H. J., and G. B. Witman. 1983. Outer doublet heterogeneity reveals structural polarity related to beat direction in *Chlamydomonas* flagella. *J. Cell Biol.* 97:902–908.
9. Huang, B., G. Piperno, and D. J. L. Luck. 1979. Paralyzed flagella mutants of *Chlamydomonas reinhardtii* defective for axonemal microtubule arms. *J. Biol. Chem.* 254:3091–3099.
10. Kamiya, R., and G. B. Witman. 1984. Submicromolar levels of calcium control the balance of beating between the two flagella in demembranated models of *Chlamydomonas*. *J. Cell Biol.* 98:97–107.
11. Laemmli, U. K. 1970. Cleavage of structural proteins during the assembly of the head of bacteriophage T4. *Nature (Lond.).* 227:680–685.
12. Luck, D., G. Piperno, Z. Ramanis, and B. Huang. 1977. Flagellar mutants of *Chlamydomonas*: studies of radial spoke-defective strains by dikaryon and revertant analysis. *Proc. Natl. Acad. Sci. USA.* 74:3456–3460.
13. Martin, R. G., and B. N. Ames. 1961. A method for determining the sedimentation behaviour of enzymes: application to protein mixtures. *J. Biol. Chem.* 236:1372–1379.
14. Pfister, K. K., R. B. Fay, and G. B. Witman. 1982. Purification and polypeptide composition of dynein ATPases from *Chlamydomonas* flagella. *Cell Motil.* 2:525–547.
15. Piperno, G., and D. J. L. Luck. 1979. Axonemal adenosine triphosphatases from flagella of *Chlamydomonas reinhardtii*. *J. Biol. Chem.* 254:3084–3090.
16. Piperno, G., and D. J. L. Luck. 1981. Inner arm dyneins from flagella of *Chlamydomonas reinhardtii*. *Cell.* 27:331–340.
17. Randall, J. T., J. R. Warr, J. M. Hopkins, and A. McVittie. 1964. A single gene mutation of *Chlamydomonas reinhardtii* effecting motility: a genetic and electron microscopic study. *Nature (Lond.).* 203:912–914.
18. Sager, R., and S. Granick. 1953. Nutritional studies with *Chlamydomonas reinhardtii*. *Ann. NY Acad. Sci.* 56:831–838.
19. Taussky, H. H., and E. Shorr. 1953. A microcolorimetric method for the determination of inorganic phosphorus. *J. Biol. Chem.* 202:675–685.
20. Van Winkle-Swift, K. P. 1977. Maturation of algal zygotes: alternative experimental approaches for *Chlamydomonas reinhardtii* (Chlorophyceae). *J. Phycol.* 13:225–231.
21. Warner, F. D. 1978. Cation-induced attachment of ciliary dynein cross-bridges. *J. Cell Biol.* 77:R19–R26.
22. Witman, G. B., J. Plummer, and G. Sander. 1978. *Chlamydomonas* flagellar mutants lacking radial spokes and central tubules. *J. Cell Biol.* 76:729–747.
23. Wray, W., T. Boulikas, V. P. Wray, and R. Hancock. 1981. Silver staining of proteins in polyacrylamide gels. *Anal. Biochem.* 118:197–203.